Physica Scripta. Vol. T41, 45–50, 1992.

Interchannel Interactions and Relaxation in the 2p Auger Spectra of Mg-like Ions

S. Fritzsche and B. Fricke

Department of Physics, University of Kassel, D-3500 Kassel, Heinrich-Plett-Str. 40, Germany

Received September 2, 1991; accepted November 6, 1991

Abstract

Relativistic Auger rates for the $2p$ spectra of Mg-like ions have been calculated in the atomic range $13 \leqslant Z \leqslant 36$. We used the multiconfiguration Dirac–Fock method but beyond a simple frozen-orbital approach we include also relaxation for the bound electrons and the interchannel interaction between the continuum states. Both effects may alter the individual transition rates remarkably. This is analysed for a few selected states within the isoelectronic sequence. Weak transitions within the $2p$ spectra can be changed by an order of magnitude because of the continuum coupling. The influence of both effects for higher-Z ions is reduced but still remain visible.

1. Introduction

The accurate study of free-atom Auger spectra involving electrons from the valence or the neighbouring closed shell is a difficult task both theoretically and experimentally. Those spectra are usually dominated by correlation and coupling effects. Because of the fast transitions the excitation and decay process often cannot be separated completely. Even in cases where these two processes are independent (i.e. a two-step model can be employed) a large number of individual transitions occur which correspond to the coupling of the open outer shells and the outgoing electrons.

Furthermore, from the view of a realistic many-body description, a detailed theoretical study may provide, by comparison with measured spectra, a sensitive test of our insights on the atomic structure and on the dynamics of the radiationless decay. A first step in this understanding is the prediction of the energies and line intensities.

During previous years quite a few experiments have been performed in light and medium Na- and Mg-like ions [1–6]. However, for the L-shell Auger spectra only recent measurements yielded a reasonable resolution of groups or sometimes even individual transitions. This was facilitated in Al^+ ions by photoinduced excitation [3], and for Ar^{6+} by ion–atom collisions [5]. A low energy line group in these spectra was first interpreted by Stolterfoht [7] as a three-electron transition indicating that configuration interaction plays a significant role.

In collision experiments the $2p$ Auger spectra have been studied also for Na-like Ar^{7+} and Fe^{15+} ions [6]. The fast ions in such collisions reduce the Doppler shift and enhance the energetic resolution in the recorded spectra. Using light atoms the variety of the usually obtained final states may be decreased remarkably.

For Mg-like ions the $2p$ Auger spectra are divided into separate peak groups and identification of the observed lines can be constructively supported by multiconfiguration Hartree–Fock calculations or its relativistic Dirac–Fock (DF) counterpart. But even in the intermediate coupling scheme the computation of transition rates do not turn out satisfactorily. Theoretically intensity ratios may deviate up to a factor of three or even more. Hence, Focke *et al.* [5] conclude from their comparison of the measured relative intensities with simple MCDF results in Ar^{6+} ions that interchannel interactions between the continuum states could be useful for explaining these discrepancies.

Similar difficulties have been known for a long time from the Ne K–LL spectrum. Howat's (nonrelativistic) investigations [8] showed that in addition to an appropriate coupling scheme the electron relaxation and intercontinuum coupling has to be taken into account. Although neon is one of the simplest atoms in this respect.

We will report here on a systematic transition rate calculation for the $2p^5 3s^2 3p$ states in Mg-like ions. Beyond the multiconfiguration Dirac–Fock (MCDF) model we include the nonorthogonality of the electron orbitals in the initial and final states as well as the continuum interaction of the decay channels. In our relativistic frame we study both effects along the Mg-isoelectronic sequence up to Kr^{24+} ions. For heavier elements the relativistic corrections to the instantaneous electron–electron interaction become dominant. This Breit interaction was recently explored by Chen for a variety of atomic transitions (see Ref. [9]) and also for the above spectra in sodium like ions [10]. Similar studies showed that configuration interaction (CI) have a strong influence on the systematic trends through the isoelectronic sequences [10, 11], especially where level crossing occur. In our approach most of the relativistic effects are included in the computations but we will not consider these effects separately from the other.

2. Theoretical method

Besides the simple perturbation approach (usually employed in practical calculations) the theoretical formulation of the Auger decay from the view of a scattering process has been presented by Åberg and Howatt [8, 12]. To include the configuration interaction between an (isolated) quasi-discrete state ψ_i and various autoionization continua $\{\psi_{\beta\tau}\}$ which are degenerate with ψ_i an additional principal value integration P along the free-electron energy has to be carried out. In the lowest order of the interaction matrix between the different continuum states

$$V_{\alpha\beta}(\varepsilon, \tau, E) = \langle \psi_{\alpha\varepsilon} | H - E | \psi_{\beta\tau} \rangle - \delta_{\alpha\beta}\, \delta(\varepsilon - \tau)(\tau + E_\beta - E) \qquad (1)$$

the partial Auger rate for a transition from initial hole-state ψ_i to the continuum state $\psi_{\alpha\varepsilon}$ is given by

$$T_{\alpha i} = 2\pi \left| \langle \psi_{\alpha\varepsilon} | H - E | \psi_i \rangle + P \sum_{\beta=1}^{N} \int_0^\infty \frac{V_{\alpha\beta}(\varepsilon, \tau, E) \langle \psi_{\beta\tau} | H - E | \psi_i \rangle}{E - E_\beta - \tau} \, d\tau \right|^2 . \quad (2)$$

This form takes also into account the correct boundary conditions for ionization processes as ingoing waves. The indices ε and τ in eqs. (1) and (2) denote the kinetic energies of the Auger electron and the electron in an intermediate continuum state, respectively. The quantity E is the total energy of the atomic system and its value is usually very close to that of the quasistationary energy E_i of ψ_i when the CI with the radiationless continua is neglected. We use atomic units throughout this paper unless specified otherwise.

Since the Auger decay is a two-electron transition, the full Hamiltonian in the transition operator $(H - E)$ is reduced to the two-electron interaction in the frozen orbital approximation. In the absence of the continuum coupling the transition rates correspond to Wentzel's ansatz [13] [first part in eq. (2)]. In most cases we used the instantaneous Coulomb repulsion for the two-electron interaction $\hat{v}_{12}$ but in some (indicated) computations we also employed the sum of Coulomb- and transverse Breit operator

$$\hat{v}_{12} = \frac{1}{r_{12}} - (\boldsymbol{\alpha}_1 \cdot \boldsymbol{\alpha}_2) \frac{\cos(\omega r_{12})}{r_{12}} + (\boldsymbol{\alpha}_1 \cdot \nabla_1)(\boldsymbol{\alpha}_2 \cdot \nabla_2) \frac{\cos(\omega r_{12}) - 1}{\omega^2 r_{12}} . \quad (3)$$

The $\boldsymbol{\alpha}_i$ are the Dirac matrices and ω denotes the wave number of the exchanged virtual photon. However, these relativistic effects in the transition operator play only a minor role for the $2p$ spectra in the Mg-like isoelectronic sequence reported here.

For our relativistic calculations we used MCDF wave functions [14]. An intermediate coupling scheme is taken into account by CI and diagonalization of the Hamiltonian submatrices where symmetry-adapted configuration state functions (CSF's) form the basis. In the energies of the initial and final states the coupling of the photon continuum [represented by the second and third term in eq. (3)] is included in lowest order perturbation.

With frozen orbitals in the initial and final states the Auger matrix elements may be decomposed into a sum of weighted radial integrals where the angular coefficients are obtained using Racah algebra [15]. For both, the Coulomb- and Breit-interaction computer programs are available [14] which we have used for the reduction of the matrix elements (ME's) for these so-called *unrelaxed* transition rates.

To take the more realistic electron relaxation into account it is necessary to treat the nonorthogonality of the orbital sets obtained in separate MCDF calculations of the initial and final states. This results in a large number of overlap integrals which have to be incorporated into the evaluation. In addition the one-electron operators in the Hamiltonian and the total energy E contribute to the transition amplitudes.

In more detail, atomic state functions (ASF's) in the MCDF method can be expanded in a linear combination of Slater determinants. These determinants are constructed from one-electron orbitals where for the initial and final states (on the right- and left-hand side of the ME's) different orbital sets have to be employed. These orbital sets will be denoted by $\{u_i\}$ and $\{v_i\}$, respectively.

For a general operator a matrix element expression, with respect to such constructed nonorthogonal determinants U and V, has been elaborated upon by Löwdin [16]. Following his formulae the Hamiltonian matrix between nonorthogonal states can be written as a sum of one- and two-electron matrix elements weighted by overlap factors. This decomposition corresponds to the one-electron Dirac operator $\hat{h}_1$ and the electron–electron repulsion $\hat{v}_{12}$ in the total Hamiltonian [16, 17]

$$\langle U\{u_i\} | \hat{H} | V\{v_i\} \rangle = \sum_{k,l} \langle u_k | \hat{h}_1 | v_l \rangle D_{UV}(k|l) + \frac{1}{2} \sum_{k_1,k_2,l_1,l_2} \langle u_{k_1} u_{k_2} | \hat{v}_{12} | v_{l_1} v_{l_2} \rangle \times D_{UV}(k_1 k_2 | l_1 l_2) \quad (4)$$

Here, $D_{UV}(k|l)$ and $D_{UV}(k_1 k_2 | l_1 l_2)$ denote the cofactors of the determinant $D_{UV} = \det |d_{kl}|$ built up from the nonorthogonal integrals

$$d_{kl} = \langle u_k | v_l \rangle . \quad (5)$$

In our relativistic Auger code we have developed a module for the complete expansion of an ASF in Slater determinants. It facilitates the computation of matrix elements between states of incomplete orthogonality for the different one- and two-electron operators in the Hamiltonian. Of course, this type of *relaxed-orbital* computation is very time consuming in comparison to the method mentioned above. Therefore, in this case, we have omitted the sophisticated relativistic Breit terms [cf. eq. (3)] in eq. (4). For the same reason we also used the frozen orbital approach for the large number of matrix elements in the principal value integration.

3. Calculations

For the generation of the initial and final bound orbitals we employed the atomic structure code of Grant and coworkers [14] in the average-level (EAL) scheme. In this scheme, the radial orbital functions are optimized by minimizing the averaged energy of all states in question. The atomic state vectors and their energies are obtained by diagonalizing the energy matrix including the transverse Breit interaction and estimated quantum-electrodynamic corrections. Since the energy of the initial states respectively the final states are close together, separate EAL calculations are an appropriate approach to take most of the electron correlation into account.

The $2p$ Auger spectra in Mg-like ions consist of all the energetically allowed transitions from 10 different initial atomic states with total angular momenta $J = 0, \ldots, 3$. Within the DF scheme these states arise mainly from a mixture of the initial (nonrelativistic) configurations

(i1) $2p^5 3s^2 3p$

(i2) $2p^5 3s 3p 3d$.

Transitions result in the final configurations

(f1) $2p^6 3s$

(f2) $2p^6 3p$
(f3) $2p^6 3d$.

Thus, in our relativistic frame we included 116 CSF's in the expansion of the initial states and five final CSF's (which do not interact in this case) as derived from the electron coupling of the open shells. Because of their single electron outside a closed shell these final configuration states are energetically well-separated from CSF's of the same symmetry.

The two initial configurations (i1) and (i2) have a strong CI whereas other configuration state functions (in particular $2p^5 3p 3d^2$ and $2p^5 3s^2 4p$) only weakly contribute to these initial states. Test calculations demonstrated, that these configurations provide only a portion < 0.003 of the initial-state wave functions which was similarly reported by Focke *et al.* [5] (cf. their Table 1). On the other hand, however, a recent calculation [18] has showed that also weak-mixing configurations may alter the transition rates remarkably and should not be excluded in advance.

To study the effects of interchannel interactions and relaxation in more detail here we have neglected these weak configurations in the CSF expansion of the initial states. Both effects will be presented separately. But for the reason of limited CSF basis we have only calculated the transition rates for five light and medium elements.

The energies of the outgoing electrons are obtained from the differences of the total energies for the initial and final ionic states which we had optimized separately. In addition we also estimated the energy shift of the initial states which is caused by the coupling to the autoionization continua. This configuration interaction of a discrete state embedded in the continuum with free-electron states was worked out by Fano [19]. For its estimation a principal value integration similar to eq. (2) has to be performed. We found a value of this energy shift smaller than 0.05 eV for all the considered initial states. These shifts were neglected in the transitions energies.

The Auger energies in the $2p$ spectra range from about 50 eV for Al^+ ions to 600 eV for Kr^{24+} ions. In this energy range the transition probabilities are not sensitive to deviations of 2 eV which may arise in this Δ–SCF method in comparison to experiment. Hence, we have employed the transition energies as given by the total energies and will not discuss them further.

To study the orbital relaxation we performed various calculations with frozen orbitals (from the initial state) and with those optimized in separate SCF calculations for the initial and final states. In the following these types of calculation will be called *unrelaxed* and *relaxed* Auger rates, respectively. Furthermore, we add the principal value integrals in eq. (2) to the partial transition amplitudes to explore the influence of the interchannel interaction. The employed integration method was reported elsewhere [20]. In the next section the influence of both effects on the Auger rates will be discussed for some selected transitions as well as along the isoelectronic sequence.

4. Results and discussion

The $2p$ Auger spectra in the Mg-isoelectronic sequence have been measured recently for Al^+ ions after photoexcitation [3] and for Ar^{6+} ions using a collisional excitation with He atoms [5]. Though in these experiments the resolution was clearly improved in comparison to earlier investigations [1, 2] most of the individual lines have not been resolved. Therefore, it was impossible to derive individual transition rates. A further problem concerned the unknown distribution of the initial state occupation after the excitation process. This determines the relative intensities of the various line groups. Comparison with theoretical intensities in which a statistical distribution [5] as well as one estimated from the photoelectron spectra [3] were assumed, are both unsatisfactory. Thus, the simplest way to test theoretical values would be to compare the relative intensities of the decay of one and the same (resolved) initial state to different final states.

4.1. *Various theoretical approaches for Al^+ ions*

Initially an accurate computation of the transition probabilities has to be carried out together with an analysis of various approximations. Within the outlined theoretical framework we performed a systematic study of the $2p$ spectra. We improved the physical picture in our approximations by taking into account the electron relaxation and the channel coupling in different calculations. Table I lists the transition rates for all $2p^{-1}$ initial states in Al^+ ions. These calculated values are corrected for electron relaxation during the decay as well as continuum interactions. Frozen-orbital computations were also reported earlier by Malutzki's group [3] and for Ar^{6+} ions by Focke *et al.* [5] using Cowan's [21] configuration interaction Hartree–Fock code (CIHF). In these calculations they used additional $2p^5 3s^2 np$ ($n \geq 4$) configurations to remove difficulties with the two S-states and, furthermore, they rescaled the radial exchange integrals in their Auger matrix elements by a factor of 0.9. This semiempirical procedure was not repeated by us. We present here pure *ab initio* results. To facilitate comparison we list our values in the same manner used in Ref. [3] (cf. Table 1). It can be seen that the individual probabilities deviate by orders of magnitude. This demonstrates the role of symmetry-adapted atomic states.

A comparison between various approaches for the transition rates shows, that relaxation and channel coupling may alter the rates strikingly. This is demonstrated in Fig. 1

Table I. *Calculated Auger transition rates from all initial $2p^5 3s^2 3p$ levels to the $2p^6 3l_j$ ($l_j = s_{1/2}, p_{1/2}, p_{3/2}, d_{3/2}, d_{5/2}$) final states in Al^+ ions. These Auger rates are corrected both for electron relaxation and the continuum interaction in the final states. The numbers in parenthesis are powers of 10*

Initial level	Final terms Transition probabilities in sec^{-1}				
$2p^5 3s^2 3p$	$3s_{1/2}$	$3p_{1/2}$	$3p_{3/2}$	$3d_{3/2}$	$3d_{5/2}$
$^1S_0$	3.20 (14)	6.99 (10)	1.37 (12)	1.06 (11)	9.14 (11)
$^3S_1$	1.69 (12)	5.28 (10)	2.02 (11)	1.48 (10)	1.80 (10)
$^1P_1$	2.39 (11)	4.97 (11)	1.06 (11)	1.55 (11)	9.48 (9)
$^3P_0$	8.63 (11)	2.78 (11)	8.76 (9)	2.80 (10)	1.94 (9)
$^3P_1$	1.30 (11)	7.38 (10)	4.47 (11)	1.932 (10)	3.42 (10)
$^3P_2$	9.47 (10)	2.83 (10)	6.82 (10)	9.83 (9)	5.88 (10)
$^1D_2$	2.54 (11)	4.77 (10)	4.51 (11)	2.69 (10)	8.74 (10)
$^3D_1$	1.45 (11)	3.68 (11)	1.75 (11)	4.99 (11)	1.30 (10)
$^3D_2$	7.88 (11)	1.76 (11)	2.41 (11)	4.38 (11)	4.85 (10)
$^3D_3$	9.62 (11)	3.31 (10)	2.28 (11)	4.94 (9)	3.00 (11)

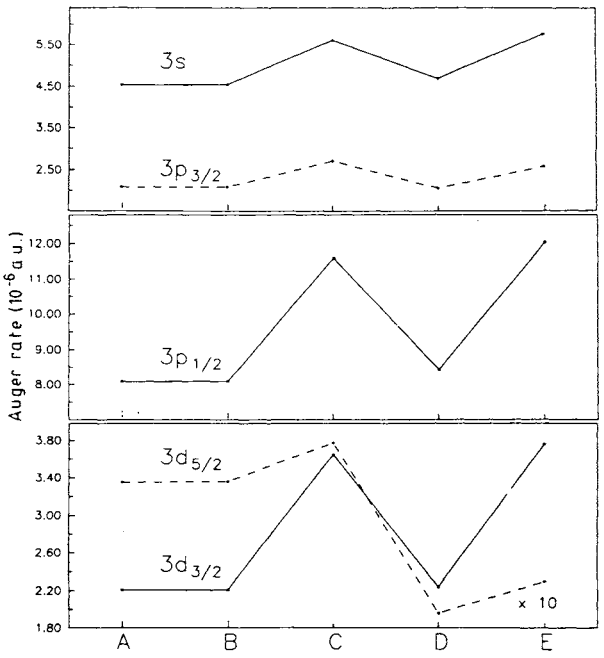

Fig. 1. Comparison of various theoretical approaches for the Auger rates of the $2p^5 3s^2 3p\ ^1P_1$ state in Al^+ ions. This hole-state may decay to the indicated $2p^6 3l_j$ ($l_j = s_{1/2}, p_{1/2}, p_{3/2}, d_{3/2}, d_{5/2}$) final states. Simple frozen-orbital MCDF calculations with only the static Coulomb-interaction in the matrix elements (A) will be shown together with similar computations including also the relativistic (transverse) Breit interaction in the transition operator (B). C represents relaxed transition rates taking into account the incomplete orthogonality of the electron orbitals in the initial and final states. Finally, D and E involve the corrections for the continuum coupling [cf. eq. (2)] with respect to the results in columns A and C, respectively. Thus, the values in the last column D may be considered to be the best

for the decay of the $2p^5 3s^2 3p\ ^1P_1$ state where the deviations between the various approaches can be seen. Besides the simple MCDF results in column A, the next column B shows that relativistic terms in the transition operator, i.e. the Breit terms in the two-electron interaction, does not change the rates in the Al^+ case.

It becomes obvious that for these $^1P_1$ transitions, the nonorthogonality of the electron orbitals (C) mostly enhances the Auger rates and the effects of this nonorthogonality is more striking than continuum interactions, except for the weak decay to the $2p^6 3d_{5/2}$ final state. Here, the channel coupling provides the dominant correction (D). For the transitions to $2p^6 3p_{1/2}$ and $2p^6 3d_{3/2}$, for example, electron relaxation increases the rates by a factor of about 1.5. However, these two effects on the frozen-orbital picture can also (partly) cancel out each other as demonstrated in Fig. 2 for Al^+ ions.

The peak group on the low-energy side of the $2p$ Auger spectra in Mg-like ions was first identified by Stolterfoht and coworkers [7] as a three-electron transition to the $2p^6 3d$ final states. In their experiment they recorded an energy pattern which was very similar to that of the two line groups which correspond to $3s$ and $3p$ transitions [5]. These transitions to the $2p^6 3d$ final states are forbidden in the single configuration approximation. Within the multiconfiguration method they become possible because of the configuration mixing of the initial configurations (i1) and (i2). In the calculation of the Auger rates these transitions to the $2p^6 3d$ final states are particular sensitive to the electron relaxation and the channel coupling as shown in Fig. 1. Furthermore, it becomes clear that even weakly contributing configurations may cause remarkable decays.

4.2. *Along the isoelectronic sequence*

For higher ionized atoms most previous calculations start with the assumption that the refinements discussed above as well as the effect of the exchange interaction between the bound and the outgoing electrons result only in slight changes of the transition probabilities. Though their influence is certainly reduced with increasing Z it is interesting to explore to which extent these effects become negligible.

For atomic zinc, for instance, we found recently a clear reduction of the L_1 Coster–Kronig decay rates due to the (inhomogeneous) exchange potential in the Dirac–Fock equations of the continuum spinor. Similar shifts have been found by Karim [17] for the argon $L_1 - L_{23}M$ Coster–Kronig spectrum.

Therefore, we have investigated the $2p$ spectrum in the Mg-like sequence up to Kr^{24+} ions and although we only computed the transition rates for five selected species the expected behaviour for an increasing nuclear charge became visible.

The various initial levels for light ions can be clearly classified by using LSJ coupling. Owing to the stronger mixing of the different configurations a simple extension to medium Z elements is not feasible. However, we employed the same notation for all considered ions using an energy ordering of the different states with the same angular momentum. Thus, levels of like symmetry will not cross each other in our notation.

In general the deviations from simple frozen-orbital calculations become smaller within the isoelectronic sequence. This applies to all considered transitions of this spectrum. However, changes due to the channel-coupling diminish faster than electron-relaxation effects. In our example, these sophisticated improvements result for Kr^{24+} ions in small corrections only and for higher Z ions the MCDF method evidently provides a reliable approximation. For even higher Z, of course, the relativistic influence becomes dominant. As described above, we used relativistic wave functions, thus including the major part of relativistic effects. But to be consistent with relaxed-orbital calculations corrected for continuum interactions we employed only the Coulomb repulsion in the transition operator. At least for the light ions up to Ar^{6+} this is a suitable approach. For heavier elements the deviations due to a relativistic Hamiltonian are then slowly increased.

Figure 2 displays the Auger rates in different approximations for the $2p^5 3s^2 3p\ ^1S_0 - 2p^6 3p\ ^2P_{1/2}$ transition. Frozen-orbital MCDF results will be shown together with relaxed Auger rates and values which involve additional contributions from interchannel interactions.

Usually relative intensities may be derived more easily from experiment than absolute transition rates. Even for an unknown population of the initial states the relative intensities for transitions to different final states can be obtained. Such a ratio is presented in Fig. 3 for the total (radiationless) decay rates of a $^1P_1$ to a $^3P_1$ state. For both $J = 1$ hole states we add the various probabilities for decaying to one of the final states of the $2p^6 3l$ ($l = s, p, d$) configurations. The approximations compared are the same as in Fig. 2. From comparison with the previous picture (Fig. 2) it

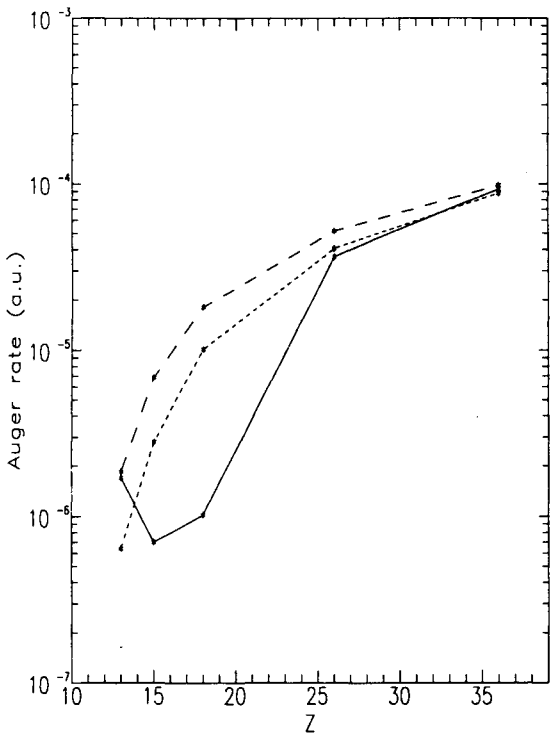

Fig. 2. Calculated Auger rates for the $2p^5 3s^2 3p\ ^1S_0 - 2p^6 3p\ ^2P_{1/2}$ transition as a function of atomic number. MCDF results with frozen orbitals (——) are compared with relaxed transition rates (– – –) including the overlap-integrals between initial and final state orbitals. The solid curve (——) represents relaxed Auger rates corrected for interchannel coupling [eq. (2)]. Theoretical values were calculated for the indicated elements; hence, all the lines connecting the data points are only for visual guidance

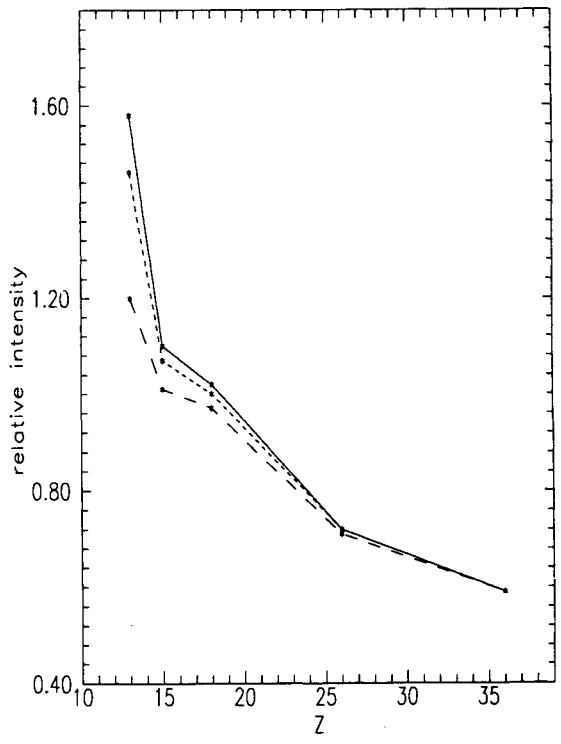

Fig. 3. Relative transition probabilities for the radiationless decay of the $^1P_1$ to the $^3P_1$ state. For both $J = 1$ hole states the total Auger rates were summed. The legend for the displayed curves are the same as in Fig. 2

is obvious that the total rates (summed up for peak groups or the hole spectra) are less sensitive than the rates for individual lines. But for the nearly neutral Al^+ ions the frozen-orbital MCDF theory is still enhanced by about 35% owing to the phenomena discussed here.

Finally, we perform a brief comparison of our theoretical values with the few experimental data available. Because of the unknown initial state population and the insufficient resolution it is reasonable to compare only intensity ratios. For the two states $^3D_1$ and $^3P_2$ these ratios (normalized to 100 for each of the $2p^{-1}$ hole state) are listed in Table II. Besides our frozen-orbital MCDF results and our best values including all the corrections for relaxation and interchannel coupling it shows the results from the CIHF calculations (using the code of Cowan [21]) and from experimental data. Although we achieve an improvement in going from unrelaxed to relaxed calculations, some deviations remain which could not be resolved in our theoretical frame. They may either be ascribed to the minimal CSF basis used or be retained further as a challenge of the electron correlation problem. On the other hand, the experimental situation does not allow a clear separation of these individual lines and, thus, the cited uncertainties may be underestimated.

5. Conclusions

For relativistic Auger rates of the 2*p* spectra of some Mg-like ions we paid special attention to the electron relaxation and the coupling of the different decay channels. The presented relaxed orbital calculations show that individual rates can be shifted remarkably because of the incomplete orthogonality of separately optimized initial and final states. Similar large deviations are caused by the continuum inter-

Table II. *Relative intensities for the decay of the $2p^5 3s^2 3p\ ^3P_1$ and $^3P_2$ hole-state to the various $2p^6 3l$ ($l = s, p, d$) final configurations. For each of the initial state the total Auger rate is normalized to 100; the given values are in %*

	$^3D_1$			$^3P_2$		
	3*s*	3*p*	3*d*	3*s*	3*p*	3*d*
Experiment[a]	6.3 ± 2	91 ± 2	2.7 ± 1	10.1 ± 1.5	80 ± 1.5	9.9 ± 1.5
Theory[b]	7	80	13	26.2	43.1	30.7
Present work (I)[c]	4.7	87.1	8.2	9.3	46.1	44
Present work (II)[d]	4.5	88.6	6.9	7.8	72.5	19.7

[a] Ref. [5]
[b] Frozen-orbital CIHF calculations [5] using the nonrelativistic code of Cowan [21]
[c] Frozen-orbital MCDF calculations within the described CSF basis (see text)
[d] MCDF results corrected for electron relaxation and channel coupling of the continuum states in eq. (2)

action of the decaying states, in particular for the strong correlated outer-shell transitions in light atoms. Of course, the most striking changes occur for weak transitions but even in faster ones the rates can be altered up to a factor of 2. Hence, relaxation and channel coupling may have the same significance as the usually considered configuration interaction of the bound states.

For higher-Z ions the relative influence of both effects become smaller but is not negligible within the investigated range. Weaker alterations usually occur for groups of lines because of the partial cancellation of the different shifts. This confirms, that total radiationless rates may be computed even in a much simpler independent-particle approximation.

Because of the scarcity of experimental data of high resolution, suitable for a separation of outer-shell transitions, a detailed comparison with measured values is not feasible. In the examples given we obtained a rough agreement which is a slight improvement compared to earlier frozen-orbital results. The remaining differences may result from our limited CSF basis and the non state-specific optimization of the initial and final atomic state functions in the EAL scheme. The large differences between the various approaches, which sometimes showed up, give an idea of the sensitivity of the transition probabilities for outer-shell transitions. To reproduce these spectra theoretically a lot of information especially for the individual transitions is necessary. In spite of these difficulties we hope that this study stimulates future experiments.

Acknowledgement

This work was supported by the Gesellschaft für Schwerionenforschung (GSI) and Deutsche Forschungsgemeinschaft (DFG).

References

1. Dahl, P., Rødbro, M., Hermann, G., Fastrup, B. and Rudd, M. E., J. Phys. **B9**, 1581 (1976).
2. Itoh, A., Schneider, T., Schiewitz, G., Roller, Z., Platten, H., Nolte, G., Schneider, D. and Stolterfoht, N., J. Phys. **B16**, 3965 (1983).
3. Malutzki, R., Wachter, A., Schmidt, V. and Hansen, J. E., J. Phys. **B20**, 5411 (1987).
4. Matsuo, T., Skibota, H., Krakowa, J., Sekiya, M., Yagiskita, A., Kombora, T., Kose, M. and Awoya, Y., J. Phys. **B21**, 1791 (1988).
5. Focke, P., Schneider, T., Schneider, D., Schiewitz, G., Kador, I., Stolterfoht, N. and Hansen, J. E., Phys. Rev. **A40**, 5633 (1989).
6. Hutten, R., Prior, M. H., Chantrenne, S., Chen, M. H. and Schneider, D., Phys. Rev. **A39**, 4902 (1989).
7. Stolterfoht, N., Schneider, T., Schneider, D. and Itoh, A., in: "Proceedings of the XIV International Conference on the Physics of Electronic and Atomic Collisions" (Abstracts, Edited by M. J. Coggiola, D. L. Huestis and R. P. Saxon) (University Press, Stanford 1985), p. 467.
8. Howat, G., Åberg, T. and Goscinsky, O., J. Phys. **B11**, 1575 (1978).
9. Chen, M. H., in: "Atomic Inner-Shell Physics" (Edited by B. Crasemann) (Plenum Press, New York, London 1985), p. 31.
10. Chen, M. H., Phys. Rev. **A40**, 2365 (1989).
11. Chen, M. H. and Crasemann, B., Phys. Rev. **A40**, 4330 (1989).
12. Åberg, T. and Howat, G., in: "Handbuch der Physik" (Edited by W. Mehlhorn) (Springer, Berlin 1982), Vol. 31, p. 469.
13. Wentzel, A., Z. Phys. **43**, 524 (1927).
14. Grant, I. P., McKenzie, B. J., Norrington, P. H., Mayers, M. F. and Pyper, N. C., Comp. Phys. Commun. **21**, 207 (1980); McKenzie, B. J., Grant, I. P. and Norrington, P. H., Comp. Phys. Commun. **21**, 233 (1980).
15. Fano, U., Phys. Rev. **140**, A67 (1965).
16. Löwdin, P. O., Phys. Rev. **97**, 1474 (1955).
17. Karim, K. R., Chen, M. H. and Crasemann, B., Phys. Rev. **A29**, 2605 (1984).
18. Hansen, J. E., private communication (1991).
19. Fano, U., Phys. Rev. **124**, 1866 (1961).
20. Fritzsche, S., Zschornack, G., Musiol, G. and Soff, G., Phys. Rev. **A44**, 388 (1991).
21. Cowan, R. D., in: "The Theory of Atomic Structure and Spectra" (Edited by David H. Sharp and L. M. Simmons, Jr.) (University of California Press, Berkeley 1981), Chap. 7-14.